

AD-774 158

UPPER-ATMOSPHERE DENSITIES DURING AN
INTENSE MAGNETIC STORM, FROM THE LOGACS
EXPERIMENT

R. R. Allan, et al

Royal Aircraft Establishment
Farnborough, England

October 1973

DISTRIBUTED BY:



National Technical Information Service
U. S. DEPARTMENT OF COMMERCE
5285 Port Royal Road, Springfield Va. 22151

ROYAL AIRCRAFT ESTABLISHMENT

Technical Report 73150

Received for printing 18 September 1973

UPPER ATMOSPHERE DENSITIES DURING AN INTENSE MAGNETIC STORM,
FROM THE LOGACS EXPERIMENT

by

R. P. Allan

G. E. Cook

SUMMARY

One of the most intense magnetic storms of recent years occurred on 25-26 May 1967 and coincided with the flight of the LOGACS (Low-G Accelerometer Calibration System) experiment aboard an Agena vehicle in a near-polar orbit. The accelerometer gave density values with an estimated accuracy better than 10% and a time resolution of 1 s, although at much longer and irregular intervals.

The day-side response (at 10.30 LT) is clearest as the geomagnetic index a_p starts to decline, and shows peaks on the magnetic equator, near $\pm 45^\circ$ geomagnetic latitude, and near the polar caps. There are pronounced troughs near $\pm 60^\circ$ geomagnetic latitude; in the northern trough (at 150 km height) the density falls to 70% of the undisturbed value. In succeeding passes the structure collapses irregularly. The equatorial peak nearly disappears within 3 h. At the peaks the density is near its maximum as a_p starts to decline, indicating a very rapid response; but the density in the troughs increases for some hours as the structure collapses, before the atmosphere returns to normal.

We suggest that the structure shows where the energy is injected, at least in the morning sector, in an intense storm, namely: (i) near the magnetic equator, (ii) near the particle precipitation zones, which are displaced equatorwards in the storm, (iii) over the polar caps. Most of the energy input is probably due to particle precipitation. The conclusion of DeVries, that most of the heating occurs in two bands around the nightside at about $\pm 70^\circ$ geomagnetic latitude, and that the energy is transported over the rest of the earth by atmospheric circulation and gravity waves, is not confirmed.

Departmental Reference: Space 444

CONTENTS

	<u>Page</u>
1 INTRODUCTION	3
2 PREFERRED NUMBERS	5
3 A STANDARD QUIET-TIME DENSITY	7
4 RESPONSE OF THE DAYTIME ATMOSPHERE	8
5 POSSIBLE HEATING MECHANISMS	11
6 CONCLUSIONS	12
Acknowledgments	15
References	16
Illustrations	Figures 1-5
Detachable abstract cards	-

I INTRODUCTION

On 22 May 1967, the US Air Force launched into a near-polar orbit an attitude-controlled Agena vehicle carrying an extremely sensitive accelerometer^{1,2}, generally known as LOGACS (Low-G Accelerometer Calibration System). Fortunately, the most intense geomagnetic disturbance since 1960 occurred during the flight. Two class 2B solar flares and one class 3B solar flare on 23 May were followed by increased solar activity, and by greatly increased geomagnetic activity on 25-26 May. As Fig.1 shows, the 10.7 cm solar radiation flux rose steadily from 178.3 (in units of $10^{-22} \text{ W m}^{-2} \text{ s}^{-1}$) on 22 May 1967 to 213.2 on 26 May. The 3-hourly geomagnetic index a_p started to increase after revolution 41, reaching a maximum of 236 on revolution 45, falling to 154 on revolution 47, and then increasing again to 400 on revolutions 51, 52 and (part of) 53 before slowly decaying to less than 100 by revolution 62.*

The orbit was near-polar with the north-going passes on the nightside at ~ 22.30 LT, and the south-going passes on the dayside at ~ 10.30 LT. The argument of perigee was initially $\omega \approx 140^\circ$, falling to 120° , so that perigee was attained at $\sim 40^\circ$ N rising to 60° N when the satellite was moving southwards on the dayside pass. After an orbital manoeuvre during revolution 18 on 23 May in which apogee was raised by ~ 70 km, the orbit had an inclination of 91.5° , and perigee and apogee heights of 147 and 403 km respectively, which decreased to 141 and 296 km over the next three days. The lowest point on the orbit relative to the real Earth (as opposed to perigee relative to a spherical Earth) was 144.7 km at $\sim 32^\circ$ N on rev. 18 falling to 137.7 km at $\sim 41^\circ$ N on rev. 65.

The LOGACS experiment provided values of atmospheric density with a time resolution of 1 s, although at much longer intervals, and an estimated accuracy of within 10%. These values have been used by DeVries^{1,2} to study the neutral atmospheric density at quiet times, and more especially its response to geomagnetic activity.

Increases in the density of the neutral atmosphere associated with geomagnetic activity were first noted by Jacchia³ from the analysis of the drag acceleration of Sputnik 3 rocket. From a later study of Injun 3, Jacchia and

* In the LOGACS data the index a_p is given as varying continuously simply by attributing each 3h value to the centre of the interval and making a linear interpolation, as shown by the broken curve in Fig.1. The use of the resulting pseudo- a_p index has been continued in this Report.

Slowey⁴ reported that the heating* was greater by a factor of 4 or 5 near the auroral zones than at low latitudes. In later, more extensive, studies using 4 satellites and covering 80 events, Jacchia *et al.*⁵ reached more guarded conclusions. For small disturbances ($K_p < 5$) the heating rate was 15-25% greater for $|\phi| > 55^\circ$ than at lower latitudes, while for larger disturbances the heating rate was sometimes greatly enhanced in the auroral zones. The heating rate appeared to be a little larger on the nightside for $K_p < 5$, with the opposite trend for larger storms, but the scatter was so large that the difference was not significant. They also found that the atmosphere responded to geomagnetic activity rather more quickly at high latitudes with a delay $\tau = 5.8 \pm 0.5$ h for $|\phi| > 55^\circ$ (av. 65°) compared with a delay $\tau = 7.2 \pm 0.3$ h for $|\phi| < 55^\circ$ (av. 25°).

On the other hand, by analysing 200 disturbances in the altitude range 250 to 800 km using drag data from 6 satellites, Roemer⁶ concluded that the time delay was independent of latitude, height or local time; on average the maximum density occurred 5.5 ± 0.3 h after the maximum geomagnetic disturbance. He also found, however, that the temperature increase was greater at higher latitudes, and also somewhat greater ($\sim 30\%$) by night than by day.

It must be pointed out that results based on orbital analysis necessarily involve averaging over a few orbits, as well as over a range of height and latitude, and therefore could well contain an intrinsic time delay. In the LOGACS experiment, it was possible to compare¹ the *in situ* acceleration data with orbital analysis based on radar observations with the conclusion that the atmospheric response deduced from orbital analysis has an inherent delay of about 3 h. Although the authors^{5,6} might not agree, it could well be that the previously quoted values of time delay should be reduced by about 3 h.

Against this somewhat confused background of results on a presumably complex phenomenon, DeVries^{1,2} came to the following conclusions from his analysis of the LOGACS data:

- (i) During quiet times the density is lower ($\sim 10\%$) than expected in the nighttime (north) auroral regions and higher ($\sim 30\%$) in the daytime (north) auroral regions.

* The increased density appears to, or is presumed to, depend on height in much the same way as would the unperturbed density for a higher level of solar activity (as measured by the F10.7 index, which is assumed to be an indicator of the intensity of the solar EUV flux); the change in density can then be expressed in terms of an equivalent change in exospheric temperature, T_e , using an atmospheric model.

- (ii) The density in the night-time (north) auroral regions increased almost simultaneously with the increase in geomagnetic activity - certainly with a delay less than 90 m (one orbital period). At the same time the density suffered a temporary decrease by up to 30% in the daytime (north) auroral regions.
- (iii) The delay time was latitude-dependent, increasing from nearly simultaneous in the night-time auroral regions to from 4½ to 6 h in the dayside equatorial regions.

DeVries concluded that most of the energy provided to the atmosphere during enhanced geomagnetic activity was deposited in the nightside auroral regions, in fact by Joule heating at or below 150 km, and transported from there by convective circulation and/or atmospheric waves. Moreover he interpreted wavelike patterns of density variation, with wavelengths of the order of 450 km and half-amplitudes of up to 35%, as evidence in favour of energy transfer by horizontally-propagating waves. The aim of the present study was to make an independent examination of the LOGACS data and in particular the evidence for atmospheric waves.

2 PREFERRED NUMBERS

In order to organize and assess the data (which had been stored on magnetic tape) we attempted to remove the height-dependence of the density without recourse to a detailed atmospheric model, by assuming that the density scale height increased linearly with height, taking the density and the scale height to have fixed values at 90 km, namely $\rho_{90} = 3.46 \times 10^{-9} \text{ g cm}^{-3}$ and $H_{90} = 5.535 \text{ km}$. The validity of this assumption of constant dH/dz can be judged from Fig. 3 for geomagnetically quiet times above 140 km. A measured density ρ at some height z can then be converted to a density ρ^* at some standard height z^* , which was taken in fact to be 140 km - near the actual height of perigee. The values of the reduced density ρ^* were then plotted (by automatic graph-plotting) for each dayside and nightside pass separately. There was in fact a dip in ρ^* around the actual perigee (on dayside passes) indicating either that dH/dz changes significantly below 140 km, or that the fixed values at 90 km are wide of the mark. The graphs, however, admirably served their purpose of assessing the data.

The graphs contained a number of seemingly artificial features which were found to be related to particular values of density in the original data. The

most striking instance occurred on the nightside pass between revs. 41 and 42 at heights approaching 350 km. Although DeVries^{1,2} would assume that all measurements above 300 km were suspect, it will serve admirably as an example.

Thus the density values contained the following sequence of numbers (all $\times 10^{-14}$ g cm⁻³):

0.412, (0.425), 0.412, 0.309, 0.258, 0.206, (0.200), 0.206, 0.258, 0.309, 0.412, 0.515, (0.590), 0.515, 0.412, 0.309, (0.307), 0.309, 0.412, 0.515, (0.696), 0.773

Clearly the same set of numbers (ignoring those in brackets) is being repeated. A count of all (roughly 6000) density values, taking the 3-digit part 0.abc and ignoring the exponent, showed that the numbers 0.103, 0.129, 0.155, 0.206, 0.258, 0.309, 0.412, 0.515 and 0.773 (and possibly also 0.121, 0.122 and 0.123) appeared much too frequently. Since there might be a 'quantisation' effect associated with measuring very low densities at the greatest heights, the counting process was repeated for each exponent separately with the values given in the form 0.abc $\times 10^{-N}$ (g cm⁻³). Some selected parts of the resulting frequency count are shown in Table 1.

Table 1 - Frequency of density values†

abc	N = 11	N = 12	N = 13	N = 14	N = 15
102	5	6	6	0	0
<u>103</u>	<u>26</u>	<u>31</u>	<u>46</u>	2	0
104	10	3	3	0	0
<hr/>					
120	7	4	3	0	0
<u>121</u>	4	<u>34</u>	4	0	0
<u>122</u>	4	<u>50</u>	5	0	0
<u>123</u>	3	<u>44</u>	3	1	0
<u>124</u>	10	9	4	0	0
128	9	3	3	0	0
<u>129</u>	<u>29</u>	<u>29</u>	<u>45</u>	3	0
130	8	4	1	0	0

† Densities are given in the form $0.abc \times 10^{-N}$ g cm⁻³

The conclusion is that the preferred numbers 103, 129, 155, 206, 258, 309, 412, 515 and 773 are associated with all exponents; those underlined are multiples of 103, and the remainder are related to them as nearly as possible as the ratio of small integers. For example

$$258 = 2 \times 129 = \frac{5}{2} \times 103 = \frac{1}{2} \times 515 = \frac{1}{3} \times 773, \text{ etc.}$$

This count also confirms the possible triplet already noted (namely 121, 122, 123) and also reveals two further triplets 151, 152, 153 and 181, 182, 183; all three triplets appear much too frequently but only in association with one exponent, namely 10^{-12} .

These preferred numbers, 18 altogether, account for over 1000 of the roughly 6000 density values. They occur most often in the earlier undisturbed portion of the data before the geomagnetic storm, where they often appear as quite 'reasonable' and 'realistic' values; the effect is that some of the points show a too exactly regular pattern of variation. Since the preferred numbers also sometimes produce features which are clearly artificial, we have chosen to reject the 'preferred numbers' everywhere.

In particular, DeVries^{1,2} has put forward wavelike patterns of density variation as evidence in favour of the transfer of energy from the auroral zones by horizontally-propagating waves. The actual patterns occur just north of the ascending nodes (on the nightside) on revs. 53 and 54 at heights between 150 and 300 km, and are shown in Fig.7 of Ref.1 (revs. 53 and 54) and in Fig.7 of Ref.2 (rev. 54 only). We find that these patterns consist largely of 'preferred numbers', and, in our opinion, cannot be accepted as evidence.

3 A STANDARD QUIET-TIME DENSITY

From the automatic plots of the 'reduced density' of section 2, it appeared that the most complete and the most structured parts of the data were to be found on the dayside passes. Accordingly we sought a more satisfactory way of quantifying the response than finding a 'reduced density'. Bearing in mind that we are concerned only with a very particular section through the atmosphere defined by local time, season (possibly) and a correlated variation of height with latitude, it seems simplest and best to find a comparison density for geomagnetically quiet times from the data of the LOGACS experiment itself. DeVries^{1,2} in fact used the densities on rev. 41, but, since the characteristics of the orbit (local time, perigee position, eccentricity) change little over the four days, it is possible to combine all the data from the first 41 orbits. Fig.2 shows all 1718 values of $\log \rho$ plotted against height from the dayside passes (defined by local time lying between 9.9 and 11.5 h) up to revolution 41, with only the 'preferred numbers' omitted. Clearly the density is a 'good' function of height only, with little scatter below about 250 km, although the passes include some with slight to moderate geomagnetic activity (a maximum of $a_p = 31$ on rev. 33).

The lowest heights from 140 to 170 km refer to the region around perigee from the equator to the (north) daytime auroral zones, while the greatest heights are attained approaching the South Pole. An inspection of the plots of 'reduced density' shows that the scatter above 250 km arises because the density polewards of about 40° S is extremely variable from pass to pass. For example the 'reduced density' approaching the South Pole shoots up on rev. 34 and falls to nearly zero on rev. 35. This variability does not seem to be correlated with any variations in a_p . Indeed it is possible that these features should be treated as fictitious. Certainly the density patterns often seem too regular for comfort, and DeVries^{1,2} would reject all measurements above 300 km as suspect. On the other hand this variability is not inconsistent with the results of Blamont and Luton⁷, who find that the temperature at F-region heights shows unexpected maxima in the polar regions even at geomagnetically quiet times.

All the daytime values of $\log \rho$ up to rev. 41 (with only the 'preferred numbers' omitted) as shown in Fig.2, are well-fitted by a cubic polynomial in the height; the sum of squares of the residuals is only marginally reduced in going beyond a cubic. Some of the individual quiet daytime passes have been compared with the density generated from the cubic polynomial. In fact rev. 41, which was used by DeVries^{1,2}, is the most nearly complete pass, and also corresponds very closely with the polynomial fit. Fig.3 shows the values of the density pseudo-scale height H , with error bars corresponding to $\pm 1\sigma$, derived from the cubic fit. The value of H increases, at first nearly linearly, from 20 km at 140 km height to a maximum of about 38 km at 270 km height and thereafter falls again. Since the density values refer to a particular section through the atmosphere, H is not the scale height at a given place. Thus it is not being suggested that the density scale height derived from a vertical section through the South polar regions is less than 30 km at 350 km height; instead it will lie somewhere between the value 30 km and an extrapolation of the early linear part of the curve in Fig.3. The linear part of the curve in Fig.3 is probably a good measure of the (vertical) density scale height up to mid-latitudes. Nevertheless, if the observations above 250 km can be accepted, Fig.3 indicates that the atmosphere in the South polar regions in May is on balance colder (although on some passes it is hotter).

4 RESPONSE OF THE DAYTIME ATMOSPHERE

The greatest and the most clearly developed response of the daytime atmosphere occurs just after the main peak of the geomagnetic storm when a_p reaches

400 for 3 h (rev. 51 to rev. 53). Fortunately the daytime pass on rev. 53 gives a nearly complete coverage in latitude, and rev. 55 is even more complete. The response is shown in Figs.4 and 5 in the form of the ratio ρ/ρ_0 , where ρ_0 is the standard quiet-time density derived in section 3, plotted against geographic latitude. Fig.4 refers to the daytime pass on rev. 53, during which ρ falls from 400 to 383; there is a gap in the latitude coverage from 50° S to 80° S. Fig.5 refers to rev. 55 during which ρ falls from 306 to 276, and is essentially complete.

The two figures are very similar; excepting the gap in Fig.4, they show a wave-like pattern with a central maximum at 10° N, further maxima at 50° N and 40° S, and yet further maxima approaching the polar caps. The pattern is not symmetrical in geographic latitude, but is much more nearly symmetrical (in form if not in magnitude) in magnetic coordinates; the magnetic equator and the feet of various L-shells are marked in Figs.4 and 5. In magnetic coordinates the central peak occurs nearly at the equator, and the next peaks are near $L = 2$ in the northern hemisphere, but perhaps nearer $L = 3$ in the southern hemisphere. This slight asymmetry between north and south in the location of the peaks and troughs could be due to the greater height in the southern hemisphere; alternatively the geometry of the situation could be imposing a compromise between geomagnetic and geographic latitudes. On the other hand there is little doubt that the greater magnitude of ρ/ρ_0 in the southern hemisphere is simply due to the greater height.

Although the gross features of the response have a wave-like pattern, the gross structure is not a propagating wave. The dayside pass on rev. 54 is somewhat incomplete in coverage, but what there is lies neatly intermediate between the patterns of Figs.4 and 5. In the succeeding dayside passes, the structure collapses in irregular fashion. It is particularly noticeable that the equatorial peak has already nearly disappeared by rev. 55.

There are certainly small-scale wave-like features such as the double peak at 50° N in Fig.5, but we would hesitate to interpret them as evidence for propagating waves. Unfortunately there is not consistently enough data with sufficiently close coverage to be able to identify small-scale features on successive passes. In any case it must be remembered that each successive pass samples the atmosphere about 23° further west.

We suggest that the structure of Figs.4 and 5 shows something like the way energy is injected into the atmosphere, at least in the evening sector. In a large geomagnetic event, namely:

- (i) Near the magnetic equator.
- (ii) In the particle precipitation zones which are displaced towards the equator in a geomagnetic storm. The more intense the storm, the greater is the displacement. As already noted, this peak appears near $L = 2$ in the northern hemisphere but nearer $L = 3$ in the southern hemisphere.
- (iii) Over the polar caps.

One of the features of the atmospheric response is the appearance of pronounced troughs at about $\pm 60^\circ$ magnetic latitude, i.e. approaching northerly auroral latitudes. The northern trough appears in both Figs.4 and 5, and reaches a minimum density of only 70% of the quiet-time value at a height of 150 km. The corresponding trough in the southern hemisphere is missing on rev. 53 due to the gap in coverage, but shows clearly in Fig.5. Here the minimum value of ρ/ρ_0 is about 1.3 at a height of 270 km. Two possible reasons for these troughs are as follows:

- (i) The air has been accelerated and displaced by electrodynamic forces.
- (ii) The air is colder, due to the removal of part of its usual heat source by the displacement of the particle trapping boundaries to much lower latitudes.

In either case it is assumed that the trough at the greater height in the southern hemisphere has been 'filled-in' to some extent by spill-over from the adjacent peaks. On the other hand the densities in the troughs appear to be in agreement with the theoretical predictions of Mayr and Volland⁸. Assuming that heating takes place near the base of the thermosphere (say between 100 and 150 km), they find that the thermospheric wind circulation excited during magnetic storms removes atomic oxygen at high latitudes. The wind-induced variations in atomic oxygen exceed temperature effects below 250 km giving a reduction in density. The calculated depletion is most pronounced near 180 km where the density can decrease by a factor of 2. Above 250 km the rise in temperature predominates and the density increases.

5 POSSIBLE HEATING MECHANISMS

DeVries² discussed the possible means by which energy is deposited in the thermosphere during geomagnetic disturbances in terms of a 1-dimensional treatment by Volland⁹ in which horizontal transport of mass, momentum and energy are neglected. Volland considered three possible locations for the original heating:

- (i) Heating at the base of the thermosphere by Joule dissipation (or wave energy). Cole¹⁰, who has particularly emphasised the possible effects of Joule heating in the auroral zones, estimated that the maximum heating takes place near 150 km.
- (ii) Energy input throughout the entire thermosphere. This would correspond, in particular, to heating by particle precipitation as suggested by McIlwain¹¹, which would give a more or less uniform rise in temperature (assuming the cross-section is independent of velocity) down to the level at which the particles are stopped.
- (iii) Heating at the top of the thermosphere, which would correspond to, for instance, heating by hydromagnetic waves generated by the interaction of the solar wind with the magnetosphere as suggested by Dessler¹².

Volland⁹ concluded that the geomagnetic activity effect was due to particle precipitation into the nightside auroral zones, i.e. heat source (ii), with a subsequent distribution in latitude and longitude by conduction and atmospheric circulation. This would be in general accord with the conclusions from satellite drag observations of an enhanced response⁴⁻⁶, and a shorter time delay⁵ at high latitudes.

Since he found an immediate increase in density over the wide latitude band polewards of about 50° N on the nightside, whereas there was a decrease at 70° N on the dayside, DeVries² reached the same conclusion on the location of the original heating. He attributed the heating, however, to Volland's heat source (i) rather than (ii); to be specific, DeVries² concluded that the mechanism was Joule dissipation (at about 150 km) around the night-time auroral zones, with the energy being transported to the rest of the earth by atmospheric circulation, conduction, and gravity waves, with the emphasis perhaps on this last mechanism. He noted, however, that an immediate response over a wide latitude band on the nightside (at about 200km height) is perhaps at variance with the theoretical predictions of Chiu and Ching¹³. In studying the effectiveness of

gravity waves in distributing an energy input, e.g. from Joule heating, they concluded that there was a density time lag of 6 ± 2 h even directly above the heat source.

The present results on the dayside response in the morning sector do not support the conclusions of DeVries². As already noted, the response has a well-developed structure by rev. 53 (when ρ_p is just beginning to decrease from the maximum value of 400 attained 3 h earlier) with a peak near the magnetic equator, further peaks at about $\pm 45^\circ$ magnetic latitude, and yet further peaks approaching the polar caps. The response at the peaks appears to be near its maximum on rev. 53, so that the time delay cannot be long. On the other hand the density in the troughs continues to increase for some hours as the pattern collapses and the troughs are filled in, before the atmosphere eventually begins to return towards normality. Since the peak values of ρ/ρ_0 in the southern hemisphere exceed the corresponding peaks in the northern hemisphere (which are at lower heights), the implication would appear to be that a substantial part of the energy input must raise the temperature fairly uniformly throughout the height range, in other words that the physical mechanism is probably particle precipitation.

6 CONCLUSIONS

The original aim of the present study had been to make an independent examination of the LOGACS data, and in particular of the possible role of gravity waves as a means of transporting energy. In the event, however, our investigations have taken a rather different course. Our initial survey of all the data, taking all dayside (~ 10.30 LT) and nightside (~ 22.30 LT) passes separately, showed that the most complete and the best ordered data were to be found on the dayside passes. The dayside passes also have the advantage of showing the response in both hemispheres; this is not possible for the nightside passes since the satellite is above 300 km, where the data is sparse and unreliable, in the southern hemisphere.

The most clearly developed dayside response occurs just after the main peak of the storm. Figs. 4 and 5 show the density ratio ρ/ρ_0 , where ρ_0 is a standard quiet-time density derived from the earlier part of the LOGACS data, for rev. 53 (just as ρ_p starts to decline from its peak value of 400) and rev. 55 respectively. Rev. 54 is not shown because it is incomplete. The response is nearly symmetrical, in form if not in magnitude, in terms of

magnetic coordinates, with a peak near the magnetic equator, further peaks near $\pm 45^\circ$ magnetic latitude, and yet further peaks approaching the polar caps. There are also pronounced troughs near $\pm 60^\circ$ magnetic latitude. The northern trough (at 150km height) appears in both figures; on rev. 53 the density is only 70% of the undisturbed value, but has recovered to 85% by rev. 55. The corresponding southern trough is missing on rev. 53 due to a gap in coverage, but appears clearly on rev. 55 where the density (at a height of 270 km) has only increased by a factor of 1.3 from its undisturbed value. At the peaks, the density is near its maximum on rev. 53 indicating that the time delay in the response is relatively short. In particular the equatorial peak on rev. 53 has nearly disappeared three hours later, perhaps because ion drag offers negligible resistance to an expansion in latitude. On the other hand the density in the troughs continues to increase for some hours; in succeeding passes the structure collapses in irregular fashion - indeed 'disintegrate' might be a more apt verb.

We suggest that the day-side response simply shows where the energy has been injected into the atmosphere, at least in the morning sector, during an intense storm, namely:

- (i) near the magnetic equator,
- (ii) near the particle trapping boundaries which are displaced equatorwards in a geomagnetic storm,
- (iii) over the polar caps.

In a further paper by one of us, it will be argued that the equatorial response is related to the decay of the ring current. This conclusion is in agreement with the results of May and Miller¹⁴ on the response of the near-equatorial atmosphere (at ~ 310 km near noon local time) from the decay of the spin-rate of Ariel 2 in March-April 1964. They found that the fine structure of the density variations was more closely correlated with the index D_{st} , an hourly index based only on the horizontal H-components at low-to-middle latitude stations and which effectively measures the strength of the ring current, than with a_p .

Turning to the mid-latitude peaks, the density ratio ρ/ρ_0 is greater at the greater heights in the southern hemisphere and the peak appears just as quickly. The conclusion would appear to be that the temperature must increase fairly uniformly throughout the height range, and that a substantial part of the energy input is probably supplied by particle precipitation.

It is not surprising that orbital drag analysis has led to confusing and contradictory conclusions if the complexity of the day side response is typical. No doubt the latitude dependence of the response varies with local time since it is unlikely that the pattern of currents or the pattern of particle precipitation will be axially symmetric. Also the response might reasonably be expected to depend on, for instance,

- (i) the inclination of the magnetic dipole axis to the earth-sun line, giving a dependence on UT/longitude,
- (ii) the sense of the interplanetary magnetic field, including its north-south component,
- (iii) the magnitude of the storm.

Recently further *in situ* results, which all refer to daytime passes near 16.00 LT, have become available from two experiments on the near-polar satellite QGO 6. Taeusch *et al.*¹⁵ have studied the response during several magnetic storms (with a maximum a_p of 80) at the end of September 1969, using measurements from the neutral mass spectrometer. They found that the increase in density (at or above 400 km) was more or less confined to high latitudes with the response increasing with latitude, and the atmosphere being scarcely affected near the equator. The response was symmetric in terms of magnetic latitude, and the time lag was less than 1h polewards of $\pm 50^\circ$. Blamont and Luton⁷ also report observations covering the same period from the Fabry-Perot interferometer. Here the neutral temperature at roughly F-region heights is derived from the Doppler broadening of the 6300 Å oxygen line in the day-glow. They find that the response to geomagnetic activity is strongest in the polar regions, with a maximum temperature of about 1700 K, and the temperature increase falls off smoothly to nearly zero at the equator. They also report unexpected temperature maxima in the polar regions even at geomagnetically quiet times.

In the present study, where the LOGACS data before the storm was used to derive a comparison undisturbed density, the quiet-time density polewards of 40° S (and above 250 km) is quite variable from pass to pass and the variation does not appear to be correlated with the (slight) geomagnetic activity taking place, at least as measured by the a_p index. This variability accounts for the scatter above 250 km evident in Fig.2, and is not inconsistent with the findings of Blamont and Luton⁷. If the observations above 250 km can be accepted, the atmosphere in the south polar regions in May is on balance colder than the rest of the dayside thermosphere.

Finally, the present study has shown that the LOGACS data is imperfect in that about 1000 of the 6000 density values are accounted for by 18 'preferred numbers' out of a total of 900 possible 3-digit numbers. The details, given more fully in section 2, are quite intriguing:

- (i) 9 of the numbers are related as nearly as possible as the ratio of small integers, and appear with all possible exponents,
- (ii) the remaining 9 numbers make up 3 sets of triplets (121,122,123; 151,152, 153; 181,182,183) and appear only with one exponent.

No explanation has been discovered. These 'preferred numbers' occur most often in the earlier undisturbed part of the data, where they usually appear as 'reasonable' and 'realistic' values, but show a too exactly regular pattern of variation. These 'preferred numbers' also give obviously artificial features, however, and we have rejected them completely in our analysis. In particular the wave-like patterns of density variation just north of the equator on the nightside passes on revs. 53 and 54 which were put forward by DeVries^{1,2} as evidence for horizontally-propagating waves, consist largely of these 'preferred numbers' and, in our view, cannot be accepted. It is possible that further imperfections still remain in the data - in places there is still a tendency towards a too exactly regular pattern of variation - but this has not been proved. Since the LOGACS experiment has provided a unique opportunity to study the atmospheric response to an intense storm, it would be highly desirable to repeat the processing of the original raw data if possible.

Acknowledgments

The authors are indebted to Mr. M.R. Gordon and Mrs. V.A. Harmer (Maths Department) who were responsible for the bulk of the programming, computation and automatic graph-plotting. They also wish to thank Mr. A.W. Odell for helpful advice and assistance. Finally they are deeply indebted to Dr. L.L. DeVries whose encouragement and assistance made this study possible.

REFERENCES

<u>No.</u>	<u>Author</u>	<u>Title, etc.</u>
1	L.L. DeVries	Analysis and interpretation of density data from the low-G accelerometer calibration system (LOGACS). <i>Space Research</i> , <u>12</u> , 777-789 (1972)
2	L.L. DeVries	Structure and motion of the thermosphere shown by density data from the low-G accelerometer calibration system (LOGACS). <i>Space Research</i> , <u>12</u> , 867-879 (1972)
3	L.G. Jacchia	Corpuscular radiation and the acceleration of artificial satellites. <i>Nature</i> , <u>183</u> , 1662-1663 (1959)
4	L.G. Jacchia J. Slowey	Atmospheric heating in the auroral zones: a preliminary analysis of the atmospheric drag of the Injun 3 satellite. <i>J. Geophys. Res.</i> , <u>69</u> , 905-910 (1964)
5	L.G. Jacchia J. Slowey F. Verniani	Geomagnetic perturbations and upper atmosphere heating. <i>J. Geophys. Res.</i> , <u>72</u> , 1423-1434 (1967)
6	M. Roemer	Geomagnetic activity effect on atmospheric density in the 250 to 800km altitude region. <i>Space Research</i> , <u>11</u> , 965-974 (1971)
7	J.E. Biamont J.M. Luton	Geomagnetic effect on the neutral temperature of the F-region during the magnetic storm of September 1969. <i>J. Geophys. Res.</i> <u>77</u> , 3534-3556 (1972)
8	H.G. Mayr H. Volland	Magnetic storm effects in the neutral composition. <i>Planet. Space Sci.</i> , <u>20</u> , 379-393 (1972)
9	H. Volland	A theory of thermospheric dynamics: 2. Geomagnetic activity, 27-day variation, and semi-annual variation. <i>Planet. Space Sci.</i> , <u>17</u> , 1709-1724 (1969)
10	K.D. Cole	Joule heating of the upper atmosphere. <i>Aust. J. Phys.</i> , <u>15</u> , 223-235 (1962)

REFERENCES (concluded)

<u>No.</u>	<u>Author</u>	<u>Title, etc.</u>
11	C.E. McIlwain	Direct measurement of particles producing visible auroras. <i>J. Geophys. Res.</i> , <u>65</u> , 2727-2747 (1960)
12	A.J. Dessler	Ionospheric heating by hydromagnetic waves. <i>J. Geophys. Res.</i> <u>64</u> , 397-401 (1959)
13	Y.T. Chiu B.K. Ching	Influence of gravity waves on transient heating response of the upper atmosphere. <i>Aerospace Corp. Report TR 0059-(6260-10)-3</i> (1970)
14	B.R. May D.E. Miller	The correlation between air density and magnetic disturbance deduced from changes of satellite spin rate. <i>Planet. Space Sci.</i> , <u>19</u> , 39-48 (1970)
15	D.R. Taeusch G.R. Carignan C.A. Reber	Response of the neutral atmosphere to geomagnetic disturbances. <i>Space Research</i> , <u>11</u> , 995-1002 (1971)

Fig. I

Geomagnetic planetary 3-hour index q_p , and mean daily solar radio flux at 10.7 cm, during Logacs experiment

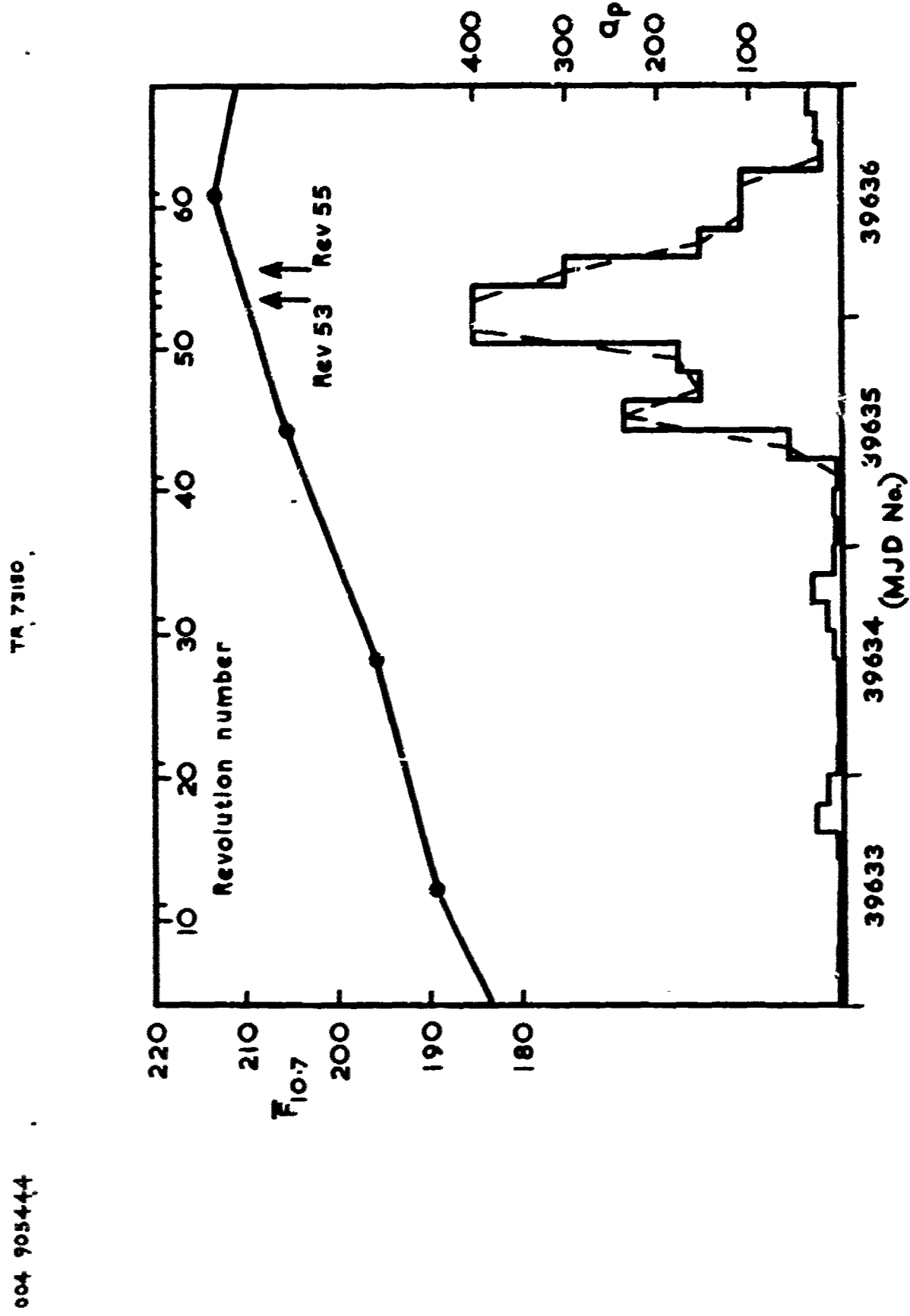


Fig. 2

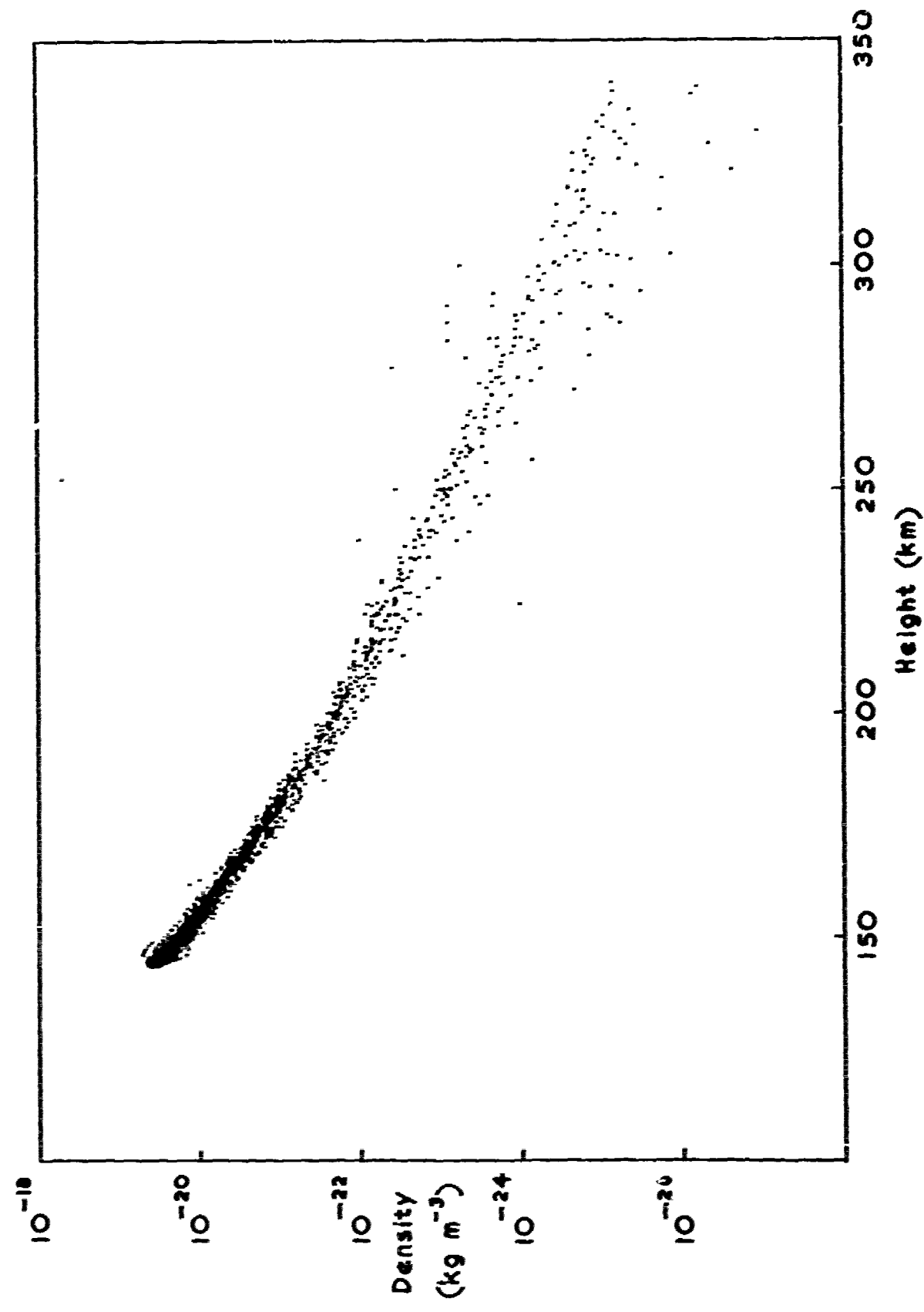


Fig. 2 Scatter plot of quiet-time dayside densities

TR, TRSP,

101431

Fig. 3

004 905445

TRA 73180

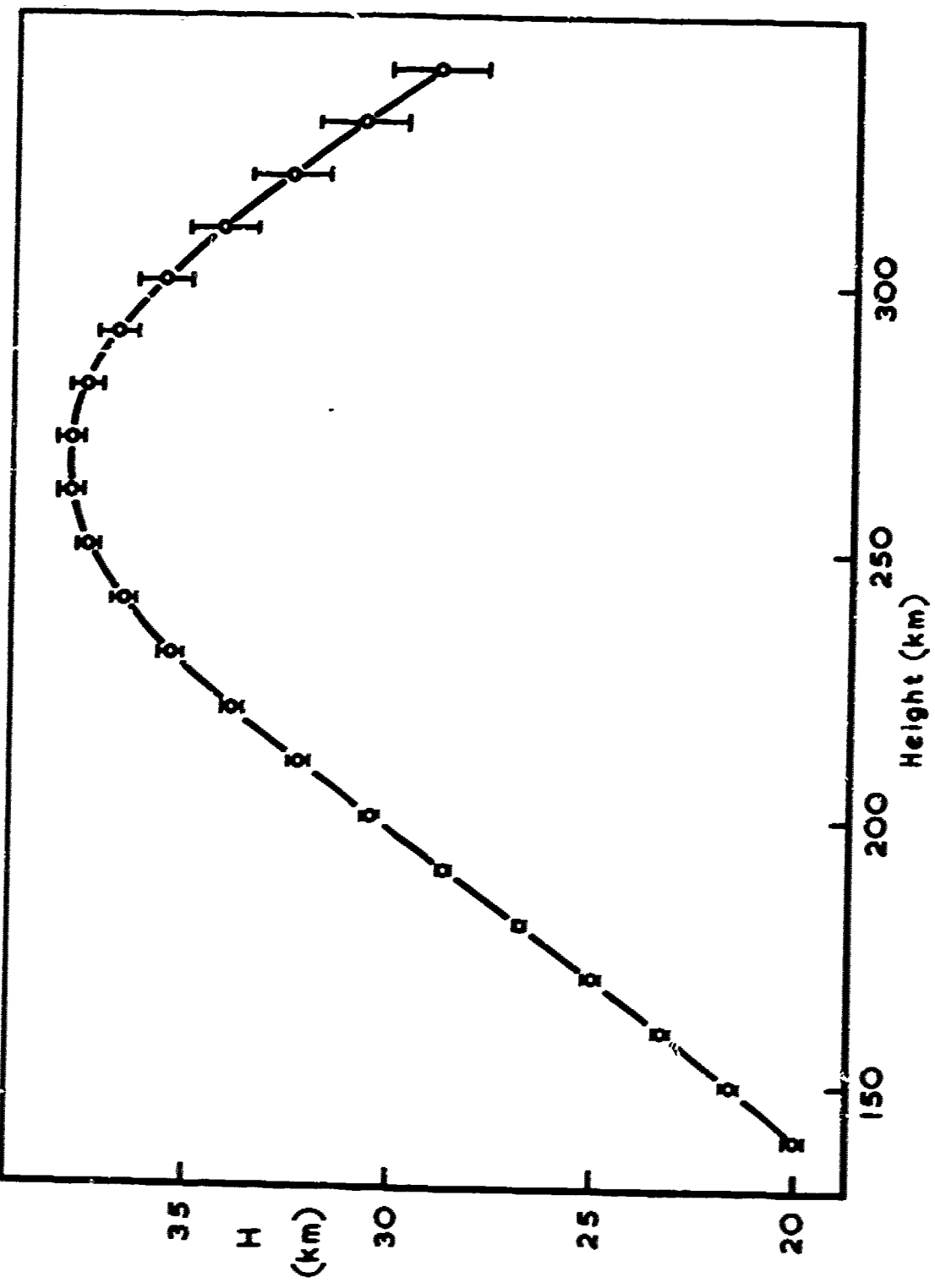
Fig. 3 Density pseudo-scale height H from quiet daytime passes

Fig.4

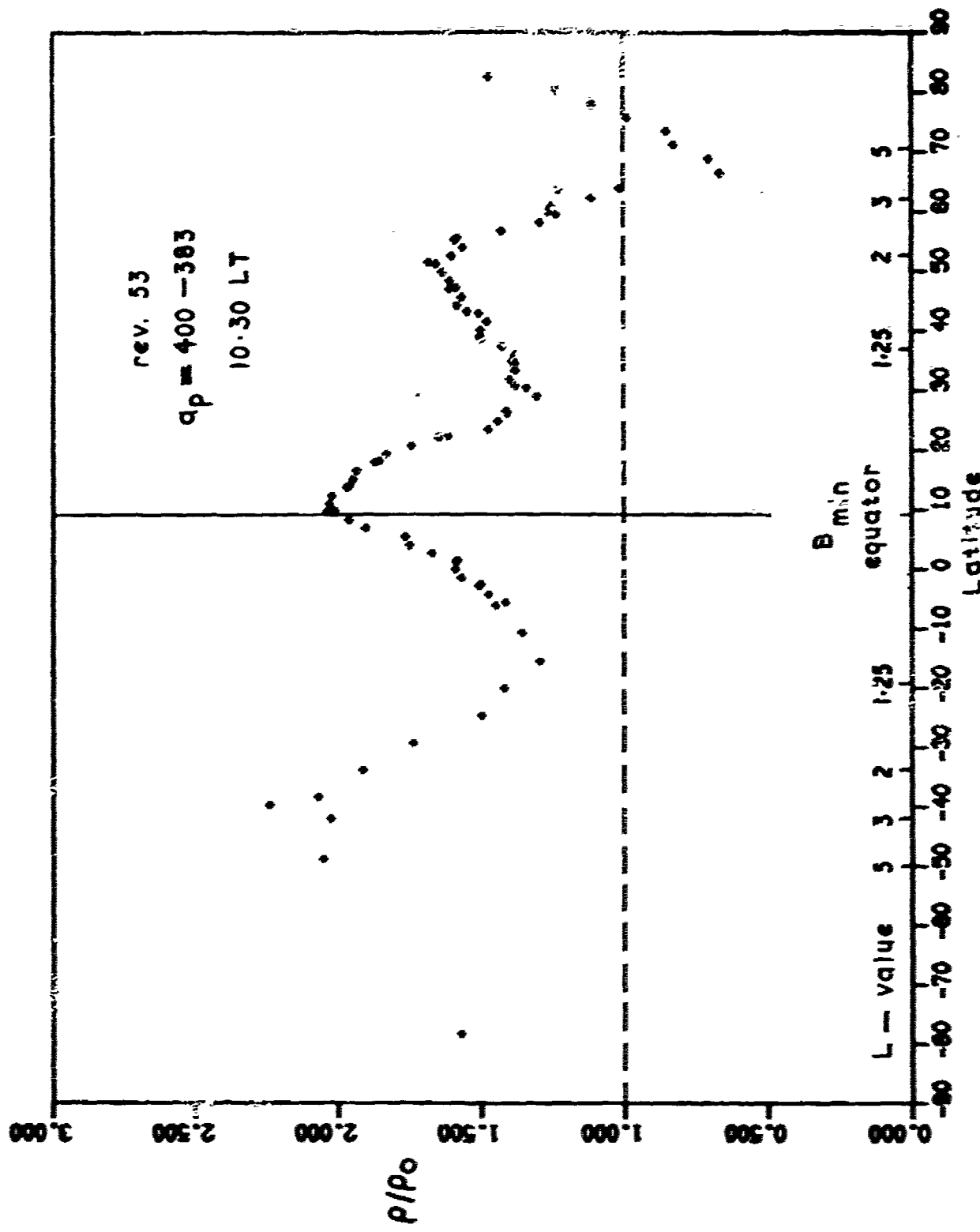


Fig. 4 Dayside density ratio for rev. 53

TM 4510

461472

Fig. 5

Fig. 5 Dayside density ratio for rev. 55

